

# Efficient State Preparation for Metrology and Quantum Error Correction with Global Control

Liam J. Bond,<sup>1,2,3</sup> Matthew J. Davis,<sup>3</sup> Jiří Minář,<sup>1,2,4</sup> Rene Gerritsma,<sup>1,2</sup> Gavin K. Brennen,<sup>5</sup> and Arghavan Safavi-Naini<sup>1,2,3</sup>

<sup>1</sup>*Institute of Physics, University of Amsterdam, Science Park 904, 1098 XH Amsterdam, the Netherlands*

<sup>2</sup>*QuSoft, Science Park 123, 1098 XG Amsterdam, the Netherlands*

<sup>3</sup>*ARC Centre of Excellence for Engineered Quantum Systems, School of Mathematics and Physics, University of Queensland, St Lucia, QLD 4072, Australia*

<sup>4</sup>*CWI, Science Park 904, 1098 XH Amsterdam, the Netherlands*

<sup>5</sup>*ARC Centre of Excellence for Engineered Quantum Systems, School of Mathematical and Physical Sciences, Macquarie University, Sydney, NSW 2109, Australia*

(Dated: December 11, 2023)

We introduce a simple, experimentally realizable protocol that can prepare any specific superposition of permutationally invariant qubit states, also known as Dicke states. The protocol is comprised entirely of global rotations and globally applied non-linear phase gates — it does not require local addressability or ancilla qubits — and hence can be readily implemented in a variety of experimental platforms, including trapped-ion quantum simulators and cavity QED systems. We demonstrate the utility of our protocol by numerically preparing several states with theoretical infidelities  $1 - \mathcal{F} < 10^{-4}$ : (i) metrologically useful  $N$ -qubit Dicke states in  $\mathcal{O}(1)$  gate steps, (ii) the  $N = 9$  qubit codewords of the Ruskai code with  $P = 4$  gate steps, and (iii) the  $N = 13$  qubit Gross codewords in  $P = 7$  gate steps. Focusing on trapped-ion platforms, we estimate that the protocol achieves fidelities  $\gtrsim 95\%$  in the presence of typical experimental noise levels, thus providing a pathway to the preparation of a variety of useful highly-entangled quantum states.

The preparation of multi-partite entangled states is essential in current efforts towards quantum advantage in quantum enhanced sensing and quantum computing. In quantum enhanced sensing, multi-partite entanglement enhances the precision of the sensor from the standard quantum limit (SQL) imposed when using an uncorrelated  $N$ -qubit state to the Heisenberg limit [1–4]. Recent impressive experimental demonstrations of the preparation of metrologically useful entangled states [5–9] highlight two limitations in the NISQ era: the fragility of multi-partite entanglement towards noise limits the fidelity of the state preparation, and the lack of single-site addressing restricts the variety of states that one can prepare to e.g. squeezed states.

The operation of a quantum computer also relies on our ability to prepare highly entangled quantum states, both as a step for quantum algorithms, and as codewords for quantum error correction (QEC). Despite recent remarkable progress towards fault-tolerant quantum computing [10–12] there are other quantum error correcting codes which may offer advantages e.g. in terms of the types of errors they can protect against [13]. One promising approach utilizes codewords which are superpositions of states in the permutationally invariant manifold, also known as Dicke states [14–16]. Dicke states are also relevant for quantum metrology [17], including error corrected quantum sensing [18], quantum storage [19, 20] and quantum networking [21]. The importance of limiting the circuit depth in NISQ devices to realize the desired state with high enough fidelity has resulted in the recent development of many state preparation proto-

cols which utilize ancilla qubits [22, 23], and shorter gate sequences interleaved with measurements and classical computation [24].

In this paper we leverage the ability to engineer infinite range interactions in quantum simulator platforms, including trapped ions and cavity QED systems, to create arbitrary superpositions of the Dicke states with applications to quantum error correction and quantum enhanced metrology. Our protocol consists of only global operations: a global non-linear phase gate and a global rotation, and thus does not demand local addressability nor ancilla qubits. We require only  $\mathcal{O}(1)$  steps to prepare metrologically useful Dicke states in tens of ions with theoretical infidelities  $1 - \mathcal{F} \sim 10^{-4}$ . Moreover, we require  $P_{\text{Ruskai}} = 4$  and  $P_{\text{Gross}} = 7$  to prepare quantum error correction codewords of the  $N = 9$  Ruskai [15] and  $N = 13$  Gross [16] codes with  $1 - \mathcal{F} < 10^{-4}$ . We discuss the possible implementation in trapped ions, including expected sources of error. The limited resources required by our protocol make it immediately realizable on a broad range of experimental quantum simulation platforms.

*Dicke states:* We consider an ensemble of  $N$  qubits. The collective spin operators are defined as  $J_\alpha = \sum_{j=1}^N \sigma_j^\alpha$  where  $\alpha \in \{x, y, z\}$  and  $\sigma_j^\alpha$  is the Pauli operator acting on the  $j$ -th qubit. The collective raising and lowering operators are  $J_\pm = J_x \pm iJ_y$ . Dicke states, denoted  $|J, M\rangle$ , are simultaneous eigenstates of the total spin operator  $J^2 = J_x^2 + J_y^2 + J_z^2$  and  $J_z$ . The quantum numbers  $J$  and  $M$  are defined by  $J^2|J, M\rangle = J(J+1)|J, M\rangle$ ,  $J_z|J, M\rangle = M|J, M\rangle$  with  $J \in \{0, \dots, N/2\}$ ,  $M \in \{-J, \dots, J\}$  taking (half)-integer values for even (odd)

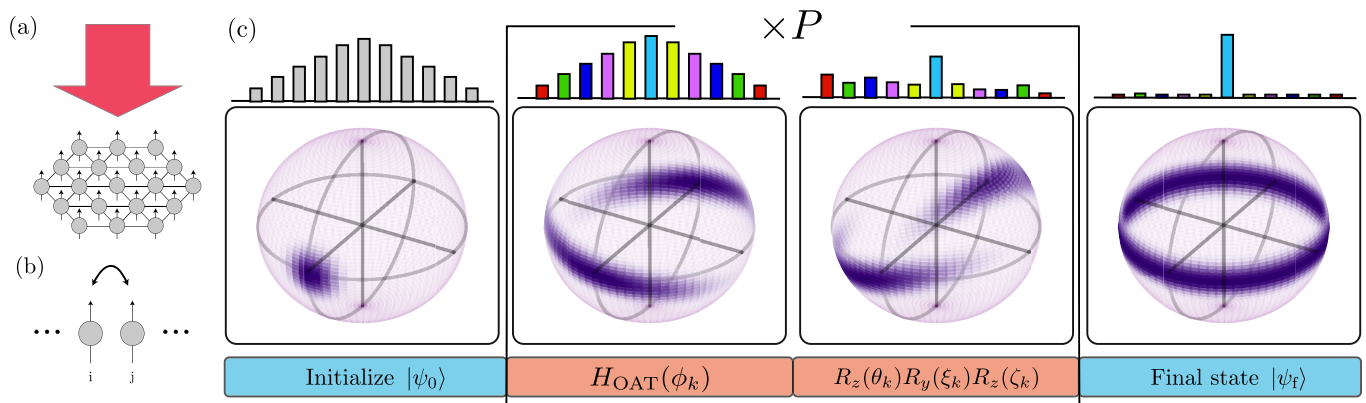


FIG. 1. (a) Our protocol utilizes operations that act globally on a collection of  $N$  qubits. (b) The Dicke states are permutationally invariant, which means that any qubits  $i$  and  $j$  can be interchanged without changing the quantum state. (c) Schematic representation of the protocol. The system is initialized in a coherent spin state (CSS)  $|\psi_0\rangle = |\bar{\theta}, \bar{\phi}\rangle$ . Next, the one-axis twisting Hamiltonian  $H_{\text{OAT}}$  generates spin squeezing. For relatively small  $\phi_k$  the CSS is spin squeezed; for larger  $\phi_k$  the probability distribution separates across the Bloch sphere, as is the case sketched here. Next, the state is rotated about an arbitrary axis. These two operations are repeated  $P$  times, with their parameters numerically optimized to maximize the fidelity between the final state  $|\psi_f\rangle$  and a chosen target state  $|\psi_t\rangle$ . Above the Bloch spheres, to highlight the protocol's relation to amplitude amplification, we roughly sketch the  $N + 1$  basis state amplitudes with colouring representing the complex phase. In this perspective,  $H_{\text{OAT}}$  applies a phase that depends non-linearly on the excitation number  $M$ , with the rotation operator then amplifying or attenuating the amplitude depending on the phase that was applied.

$N$ . In this work we focus on the symmetric  $J \equiv N/2$  Dicke states. The  $N + 1$  states in this manifold can be written in the single-particle  $\sigma_z$  basis as

$$|J = N/2, M\rangle = \frac{1}{\sqrt{\lambda}} \sum_{\mathcal{P}} (|1\rangle^{J+M} \otimes |0\rangle^{J-M}), \quad (1)$$

where the normalisation factor is  $\lambda = \binom{2J}{J+M}$ , and where the summation is over all permutations  $\mathcal{P}$  of the ordering of the spins. For example, for  $N = 3$  the four symmetric Dicke states are  $|3/2, -3/2\rangle = |000\rangle$ ,  $|3/2, -1/2\rangle = 1/\sqrt{3}(|001\rangle + |010\rangle + |100\rangle)$ ,  $|3/2, 1/2\rangle = 1/\sqrt{3}(|011\rangle + |101\rangle + |110\rangle)$  and  $|3/2, 3/2\rangle = |111\rangle$ . The entanglement of Dicke states is persistent [25], which makes them attractive for experimental realization. Dicke states such as the  $N$ -qubit W state or the Dicke state with  $N/2$  excitations are robust and demonstrate useful sensing capabilities [26–28]. There are many deterministic preparation protocols for Dicke states, including quantum circuit approaches [22–24] and global pulse schemes [29–32], among others [33–35].

In addition to bare Dicke states, superpositions of Dicke states are of key interest. For example, the Greenberger–Horne–Zeilinger (GHZ) state  $|\text{GHZ}\rangle = |N/2, -N/2\rangle + |N/2, N/2\rangle$  is maximally entangled, represents a distinct class of multi-partite entanglement and exhibits phase sensing sensitivity below the SQL [36, 37]. Its preparation has been experimentally demonstrated in platforms including trapped ions [38], Rydberg atom arrays [5] and superconducting qubits [6].

Going beyond simple Dicke states, preparation of more complicated states quickly becomes challenging. This is

particularly the case for the codewords of Pauli exchange error correcting codes [15] or the codewords of large spin codes [16] which are superpositions of Dicke states with highly specific coefficients.

*State preparation protocol:* Our protocol requires a phase gate that depends non-linearly on  $M$ . We use the one-axis twisting Hamiltonian  $H_{\text{OAT}} = gJ_z^2$  with coupling strength  $g$  [39]. The corresponding evolution operator is

$$U_{\text{OAT}}(\phi) = e^{-i\phi J_z^2}, \quad (2)$$

where  $\phi = gt$  with  $t$  the duration for which  $H_{\text{OAT}}$  is applied. We construct a gate sequence that is composed of  $U_{\text{OAT}}$  interleaved with global rotations about an arbitrary axis described by  $R(\theta_k, \xi_k, \zeta_k) = R_z(\theta_k)R_y(\xi_k)R_z(\zeta_k)$ . The resulting unitary is

$$U_{\text{tot}} = \prod_{k=1}^P [R(\theta_k, \xi_k, \zeta_k)U_{\text{OAT}}(\phi_k)], \quad (3)$$

where  $P$  denotes the number of steps. We note that in the large  $N$  limit, after making the Holstein-Primakoff transformation [40],  $H_{\text{OAT}}$  and  $R$  become a Kerr nonlinearity and displacement operator, respectively, which may open a path for other experimental implementations.

We sketch a schematic overview of the protocol in Fig. 1. The protocol design is motivated by amplitude amplification: in the computational basis  $U_{\text{OAT}}$  applies a phase that depends non-linearly on  $M$ . When the state is then rotated about a chosen axis, the amplitude of each  $|N/2, M\rangle$  is either amplified or attenuated, depending on

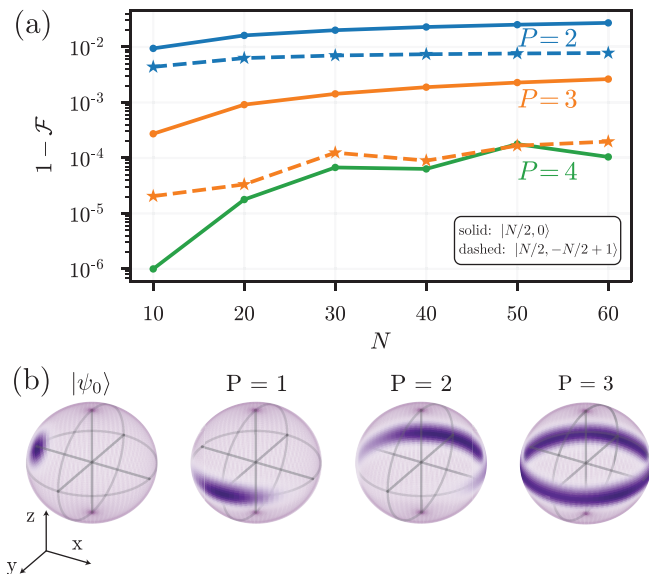


FIG. 2. (a) Theoretical infidelity  $1 - \mathcal{F} = 1 - |\langle \psi_t | \psi_f \rangle|^2$  to prepare: the  $N/2$  excitation state  $|N/2, 0\rangle$  (solid, dots) and the W state  $|N/2, -N/2 + 1\rangle$  (dashed, stars) using the protocol  $U_{\text{tot}}$  Eq. (3). Both target states, even for  $N = 60$ , can be prepared with small theoretical infidelities  $1 - \mathcal{F} \sim 10^{-4}$  in  $P = 4$  and  $P = 3$  gate steps respectively. (b) The  $\text{su}(2)$  Husimi Q-representation for the  $P = 3$  gate sequence solution that prepares  $|N/2, 0\rangle$  with  $N = 60$ . Starting with the spins pointing along  $-x$ , the interleaving of spin squeezing generated by  $H_{\text{OAT}}$  and the global rotations produces a trajectory through Hilbert space that leads to the preparation of the target state with infidelity  $1 - \mathcal{F} \sim 2 \times 10^{-3}$ . The optimized parameters used for this sequence are  $\phi = [0.054, 4.712, 3.441]$ ,  $\zeta = [0.412, 3.142, 3.096]$  and  $\xi = [4.474, 3.142, 3.115]$ .

the phase that was imparted by  $U_{\text{OAT}}$ . In this way, repeated application of  $U_{\text{OAT}}$  and  $R$  with optimized parameters can maximize the amplitude of a target state while minimizing the amplitude of all other states in Hilbert space. The parameters  $\theta, \xi, \zeta$  and  $\phi$  are chosen to minimize the infidelity  $1 - \mathcal{F} = 1 - |\langle \psi_t | \psi_f \rangle|^2$  where  $|\psi_t\rangle$  is a chosen target state,  $|\psi_f\rangle = U_{\text{tot}}|\psi_0\rangle$  the final state and  $|\psi_0\rangle$  the initial state.

Because the gate sequence Eq. (3) begins with the application of  $U_{\text{OAT}}$ , for the initial state we choose a global rotation acting on  $|N/2, -N/2\rangle$ , which is a coherent spin state (CSS)  $|\psi_0\rangle = |\bar{\theta}, \bar{\phi}\rangle$ , ie. an eigenstate of the spin component in the  $(\bar{\theta}, \bar{\phi})$  direction. The parameters  $(\bar{\theta}, \bar{\phi})$  are also numerically optimized, and thus the total number of free parameters is  $4P + 3$ .

*Dicke state preparation:* We demonstrate numerically that the protocol Eq. (3) can prepare  $N$ -qubit symmetric Dicke states with high theoretical fidelity. Our numerical optimisation uses a multi-start Monte Carlo search, with local optimisation implemented using L-BFGS [41] in JULIA [42] with OPTIM.JL and LINESEARCHES.JL [43].

Firstly, we prepare the Dicke state with  $N/2$  excita-

tions,  $|\psi_t\rangle = |N/2, 0\rangle$ . Note that this state is metrologically useful: when the state used for sensing is  $|N/2, 0\rangle$ , the uncertainty in the measured angle  $\epsilon$  of a rotation  $e^{-i\epsilon J_y}$  saturates the Cramer-Rao bound,  $(\Delta\epsilon)^2 = 2/[N(N+2)]$  and is robust to particle loss [44, 45]. We exploit the symmetry of  $|N/2, 0\rangle$  in the Dicke manifold to reduce the number of parameters by restricting the global rotations in the protocol to  $R_z(\theta_k)$  and  $R_y(\xi_k)$ , and by setting the initial CSS to be an eigenstate of  $J_x$  such that  $\langle \psi_0 | J_x | \psi_0 \rangle = -N/2$ . In Fig. 2(a) we plot (solid lines with dots) the infidelity  $1 - \mathcal{F} = 1 - |\langle \psi_t | \psi_f \rangle|^2$  as a function of  $N$  for  $P = 2$  (blue),  $P = 3$  (orange) and  $P = 4$  (green). The infidelity is remarkably robust to increasing qubit number, with  $P = 4$  gates sufficient to prepare the target state in tens of ions with infidelities  $1 - \mathcal{F} \sim 10^{-4}$ . In Fig. 2(b) we plot the evolution of the  $N = 60$  state under the  $P = 3$  gate sequence solution using the  $\text{su}(2)$  Husimi Q-Representation  $Q(\theta, \phi) = \langle \theta, \phi | \rho | \theta, \phi \rangle$  of a state  $\rho$  where  $|\theta, \phi\rangle$  is a CSS. Clearly visible is the effect of spin squeezing, whose repeated application combined with global rotations results in the preparation of  $|N/2, 0\rangle$ .

Secondly, we prepare the  $N$ -qubit W state,  $|N/2, -N/2 + 1\rangle$ . In Fig. 2(a), we plot (dashed lines with stars) the infidelity to prepare the W state as a function of  $N$  with  $P = 2$  (blue) and  $P = 3$  (orange) gate steps. Note that the superposition of all states with only one qubit not excited  $|N/2, N/2 - 1\rangle$  can be prepared using the same sequence by applying a global spin flip at the end of the sequence, and that optimizing for  $|N/2, N/2 - 1\rangle$  rather than  $|N/2, -N/2 + 1\rangle$  does not offer any potential for improvement as the initial state is an optimized CSS. Importantly, we find that the  $N = 60$  W state can be prepared with small infidelities in only  $P = 3$  gates. Thus, our protocol can be used to prepare large  $N$  Dicke states in  $\mathcal{O}(1)$  gate steps.

*Quantum error correction codewords:* Next, we demonstrate the versatility of our protocol by preparing specific superpositions of Dicke states. We focus on the codewords of the Ruskai and Gross codes.

Pauli exchange errors are two-qubit errors that arise due to interactions between qubits, which can occur for example due to dipole-dipole interactions. Physically, exchange errors are similar to bit flip errors, with the additional constraint that a qubit will flip if and only if its neighbour is different. Codes such as the 9-qubit Shor code [46] cannot distinguish between exchange errors and phase errors. The Ruskai code [15] exploits the permutation invariance of Dicke states to correct all one qubit errors and Pauli exchange errors. The explicit codewords for  $N = 9$  are

$$|R_0\rangle = |9/2, -9/2\rangle + \frac{1}{\sqrt{28}}|9/2, 3/2\rangle, \quad (4a)$$

$$|R_1\rangle = |9/2, 9/2\rangle + \frac{1}{\sqrt{28}}|9/2, -3/2\rangle, \quad (4b)$$

where the coefficient  $1/\sqrt{28}$  is required to satisfy the QEC condition [15].

As a second example, we consider the Gross codes [16]. Designed such that the logical single-qubit Clifford operations are global rotations, the Gross code is immune, to first order, to errors that correspond to global rotations. As such, the code utilizes interactions that are native to many experimental platforms, and protects against the typically most deleterious sources of noise, including both  $T_1$ -type relaxation and  $T_2$ -type dephasing errors. The smallest collective spin for which this code can be constructed is  $N = 13$ . It utilizes the two following states  $|\tilde{G}_{0,1}\rangle = c_1|13/2, 13/2\rangle + c_2|13/2, 5/2\rangle + c_3|13/2, -3/2\rangle + c_4|13/2, -11/2\rangle$ , where the coefficients for  $|\tilde{G}_0\rangle$  are  $c_1 = \sqrt{910}/56$ ,  $c_2 = -3\sqrt{154}/56$ ,  $c_3 = -\sqrt{770}/56$  and  $c_4 = \sqrt{70}/56$ ; and for  $|\tilde{G}_1\rangle$  are  $c_1 = \sqrt{231}/84$ ,  $c_2 = \sqrt{1365}/84$ ,  $c_3 = -\sqrt{273}/28$  and  $c_4 = -\sqrt{3003}/84$ . The explicit codewords are then

$$|G_0\rangle = \frac{\sqrt{105}}{14}|\tilde{G}_0\rangle + \frac{\sqrt{91}}{14}|\tilde{G}_1\rangle, \quad (5)$$

where  $|G_1\rangle$  follows from  $|G_0\rangle$  by a global spin flip, and where the coefficients are all determined by the error correction condition [16].

In Fig. (3) we plot the infidelity of the state  $|\psi_t\rangle$  after the optimized gate protocol Eq. (3) with target states  $|\psi_t\rangle = |R_1\rangle$  (blue with dots) and  $|\psi_t\rangle = |G_0\rangle$  (orange with stars). We find solutions that prepare the codewords with infidelities  $1 - \mathcal{F} < 10^{-4}$  in only  $P = 4$  and  $P = 7$  gate steps respectively. Therefore, our protocol provides a pathway towards the implementation of large  $N$ -qubit QEC codes utilizing only global addressability of the qubits constituting the codeword.

Considering system sizes of  $N \sim 100$ , we have observed that it is possible to numerically find gate sequences with  $P = \mathcal{O}(N)$  pulses with infidelities  $\mathcal{O}(10^{-6})$ . This suggests that there is an efficient protocol of at most a linear depth to prepare Dicke states with small infidelity.

*Realization in trapped ions:*  $H_{\text{OAT}}$  can be realized in trapped ions by off-resonantly driving the centre of mass (COM) mode [38, 47–50]. Considering  $N$  ions in a linear Paul trap, two global Raman beams detuned from the red and blue sidebands by  $\delta$  leads to the following Hamiltonian in the interaction picture,

$$H_I = \frac{\Omega\eta}{2}(ae^{-i\delta t} + a^\dagger e^{i\delta t})J_z, \quad (6)$$

where we have assumed the Lamb-Dicke regime, and where  $a$  ( $a^\dagger$ ) are the annihilation (creation) operators of the COM mode,  $\eta$  the Lamb-Dicke parameter and  $\Omega$  the Rabi frequency. Note that although we require the Lamb-Dicke regime, our protocol is otherwise insensitive to temperature and therefore does not require ground state cooling [47, 51]. Evolving for time  $t_f = 2\pi/\delta$  results in a closed loop in phase space such that the motion decouples from the spin degree of freedom. The effective evolution

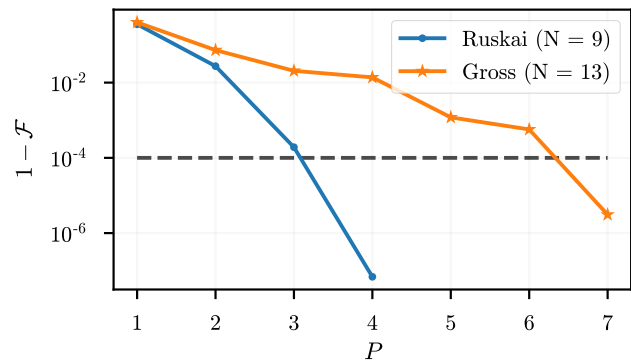


FIG. 3. Infidelity to prepare the  $N = 9$  Ruskai  $|R_1\rangle$  and  $N = 13$  Gross  $|G_0\rangle$  codewords using the optimized gate sequence as a function of gate steps  $P$ . Despite being highly specific superpositions of Dicke states, we numerically find solutions that can prepare both target states with infidelities  $1 - \mathcal{F} < 10^{-4}$  in  $P = 4$  and  $P = 7$  gate steps for  $|R_1\rangle$  and  $|G_0\rangle$  respectively.

is described by one-axis twisting,  $U_{\text{OAT}} = \exp(-i\phi J_z^2)$  with  $\phi = \pi\eta^2\Omega^2/\delta^2$  the area enclosed [52]. Our optimised solutions are typically  $\phi \sim 1$ . Setting  $\eta\Omega = 2\pi \times 20$  kHz and  $\delta = 2\pi \times 20$  kHz results in  $t_f = 50 \mu\text{s}$  and  $\phi = \pi$ . The total protocol duration  $T$  is therefore  $T = Pt_f$ , and thus for all the gate sequences we present  $T \lesssim 350 \mu\text{s}$ .

Off-resonant driving of the other modes will lead to non-uniform spin-dependent phases. Assuming a typical trap frequency  $\omega = 2\pi \times 2$  MHz, the stretch mode, which is the leading order correction, is detuned by  $(\sqrt{3}-1)\omega + \delta$ . The area enclosed by the stretch mode is  $\sim 10^{-3}$  times smaller than the area enclosed by the COM mode, and thus for realistic parameters unwanted off-resonant driving of the collective modes is negligible compared to the effects of dephasing, which we consider below.

We use a realistic dephasing rate  $\gamma = 2\pi \times 5$  Hz. The off-diagonal coherences of the GHZ state decay as  $\sim e^{-\gamma Nt}$ , such that the fidelity can be roughly estimated as  $F \sim 1/2(1 + e^{-\gamma Nt})$ . We assume that the rotations are noise-free, as they can be performed fast relative to the spin squeezing. For the  $N = 9$  Ruskai and  $N = 13$  Gross protocols, using the  $P = 4$  and  $P = 7$  gate sequences respectively, assuming the ideal protocol prepares the state with perfect fidelity, we estimate noisy fidelities  $\mathcal{F} \sim 97\%$  and  $\mathcal{F} \sim 93\%$  respectively. Reducing the dephasing rate to  $\gamma = 2\pi \times 1$  Hz increases the Ruskai and Gross codeword fidelities to  $\mathcal{F} \sim 99\%$  and  $\mathcal{F} \sim 98\%$  respectively. Furthermore, parametric amplification can increase the squeezing amplitude achieved in a given  $t_f$  [53], whilst multiple Raman beatnotes can reduce off-resonant driving enabling a larger  $\delta$  [54, 55]. Therefore such techniques, when combined with achievable reductions in dephasing noise, could bring state preparation infidelities of the Gross and Ruskai codewords below QEC thresholds

in the near-term.

*Outlook:* We proposed a few-gate protocol to prepare specific superpositions of Dicke states which can be easily realized across a variety of experimental platforms. Its implementation could lead to the preparation of interesting and useful entangled states, with applications in quantum metrology and quantum error correction.

Finally, we note that the set of realizable interactions depends on the experimental platform, e.g. in cavity QED experiments dispersive interactions can be used to engineer the generator  $\sin(J_z + \varphi)$  [29], whilst addressing the second red and blue sidebands in trapped ions can produce  $\cosh(rJ_z) + \cos(\varphi) \sinh(rJ_z)$ . These Hamiltonians can replace  $H_{\text{OAT}}$ ; or the inclusion of more than one flavour of phase gate in the protocol could provide additional geometric control, potentially reducing the total number of gate steps required.

*Acknowledgments:* We thank Dominic Berry for discussions. This work was supported by the Netherlands Organization for Scientific Research (Grant Nos. OCENW.XL21.XL21.122 and VI.C.202.051, (R.G.)), and the Australian Research Council (ARC) Centre of Excellence for Engineered Quantum Systems (EQUS, CE170100009). A.S.N is supported by the Dutch Research Council (NWO/OCW), as part of the Quantum Software Consortium programme (project number 024.003.037) and Quantum Delta NL (project number NGF.1582.22.030).

*Author's note:* While completing our manuscript we became aware of a recent preprint proposing a similar protocol [56].

- 
- [1] V. Giovannetti, S. Lloyd, and L. Maccone, *Nature Photonics* **5**, 222 (2011).
- [2] C. M. Caves, *Phys. Rev. D* **23**, 1693 (1981).
- [3] D. Wineland, J. Bollinger, W. Itano, and F. Moore, *Phys. Rev. A* **46**, 6797 (1992).
- [4] R. Kaubruegger, D. V. Vasilyev, M. Schulte, K. Hammerer, and P. Zoller, *Phys. Rev. X* **11**, 041045 (2021).
- [5] A. Omrán, H. Levine, A. Keesling, G. Semeghini, T. T. Wang, S. Ebadi, H. Bernien, A. S. Zibrov, H. Pichler, S. Choi, J. Cui, M. Rossignolo, P. Rembold, S. Montangero, T. Calarco, M. Endres, M. Greiner, V. Vuletić, and M. D. Lukin, *Science* **365**, 570 (2019), <https://www.science.org/doi/pdf/10.1126/science.aax9743>.
- [6] C. Song, K. Xu, H. Li, Y.-R. Zhang, X. Zhang, W. Liu, Q. Guo, Z. Wang, W. Ren, J. Hao, H. Feng, H. Fan, D. Zheng, D.-W. Wang, H. Wang, and S.-Y. Zhu, *Science* **365**, 574 (2019), <https://www.science.org/doi/pdf/10.1126/science.aay0600>.
- [7] H. Strobel, W. Muessel, D. Linnemann, T. Zibold, D. B. Hume, L. Pezze, A. Smerzi, and M. K. Oberthaler, *Science* **345**, 424 (2014).
- [8] J. G. Bohnet, B. C. Sawyer, J. W. Britton, M. L. Wall, A. M. Rey, M. Foss-Feig, and J. J. Bollinger, *Science* **352**, 1297 (2016).
- [9] C. D. Marciniak, T. Feldker, I. Pogorelov, R. Kaubruegger, D. V. Vasilyev, R. van Bijnen, P. Schindler, P. Zoller, R. Blatt, and T. Monz, *Nature* **603**, 604 (2022).
- [10] D. Bluvstein, S. J. Evered, A. A. Geim, S. H. Li, H. Zhou, T. Manovitz, S. Ebadi, M. Cain, M. Kalinowski, D. Hangleiter, J. P. B. Ataiades, N. Maskara, I. Cong, X. Gao, P. S. Rodriguez, T. Karolyshyn, G. Semeghini, M. J. Gullans, M. Greiner, V. Vuletić, and M. D. Lukin, *Nature* (2023), 10.1038/s41586-023-06927-3.
- [11] S. Krinner, N. Lacroix, A. Remm, A. Di Paolo, E. Genois, C. Leroux, C. Hellings, S. Lazar, F. Swiadek, J. Herrmann, G. J. Norris, C. K. Andersen, M. Müller, A. Blais, C. Eichler, and A. Wallraff, *Nature* **605**, 669 (2022).
- [12] V. V. Sivak, A. Eickbusch, B. Royer, S. Singh, I. Tsioutsios, S. Ganjam, A. Miano, B. L. Brock, A. Z. Ding, L. Frunzio, S. M. Girvin, R. J. Schoelkopf, and M. H. Devoret, *Nature* **616**, 50 (2023).
- [13] B. M. Terhal, *Rev. Mod. Phys.* **87**, 307 (2015).
- [14] Y. Ouyang, *Phys. Rev. A* **90**, 062317 (2014).
- [15] M. B. Ruskai, *Phys. Rev. Lett.* **85**, 194 (2000).
- [16] J. A. Gross, *Phys. Rev. Lett.* **127**, 010504 (2021).
- [17] G. Tóth, *Phys. Rev. A* **85**, 022322 (2012).
- [18] Y. Ouyang and G. K. Brennen, “Quantum error correction on symmetric quantum sensors,” (2023), arXiv:2212.06285 [quant-ph].
- [19] M. Plesch and V. Bužek, *Phys. Rev. A* **81**, 032317 (2010).
- [20] D. Bacon, I. L. Chuang, and A. W. Harrow, *Phys. Rev. Lett.* **97**, 170502 (2006).
- [21] R. Prevedel, G. Cronenberg, M. S. Tame, M. Paternostro, P. Walther, M. S. Kim, and A. Zeilinger, *Phys. Rev. Lett.* **103**, 020503 (2009).
- [22] A. Bäertschi and S. Eidenbenz, in *2022 IEEE International Conference on Quantum Computing and Engineering (QCE)* (2022) pp. 87–96.
- [23] S. Aktar, A. Bäertschi, A.-H. A. Badawy, and S. Eidenbenz, *IEEE Transactions on Quantum Engineering* **3**, 1 (2022).
- [24] H. Buhrman, M. Folkertsma, B. Loff, and N. M. P. Neumann, “State preparation by shallow circuits using feed forward,” (2023), arxiv:2307.14840 [quant-ph].
- [25] H. J. Briegel and R. Raussendorf, *Phys. Rev. Lett.* **86**, 910 (2001).
- [26] W. Dür, G. Vidal, and J. I. Cirac, *Phys. Rev. A* **62**, 062314 (2000).
- [27] D. Wineland, J. Bollinger, W. Itano, and D. Heinzen, *Phys. Rev. A* **50** (1994).
- [28] L. Pezzè, A. Smerzi, M. K. Oberthaler, R. Schmied, and P. Treutlein, *Rev. Mod. Phys.* **90**, 035005 (2018).
- [29] M. T. Johnsson, N. R. Mukty, D. Burgarth, T. Volz, and G. K. Brennen, *Phys. Rev. Lett.* **125**, 190403 (2020).
- [30] S. S. Ivanov, N. V. Vitanov, and N. V. Korolkova, *New Journal of Physics* **15**, 023039 (2013).
- [31] V. M. Stojanovic and J. K. Nauth, *Physical Review A* **108**, 012608 (2023), arxiv:2302.12483 [quant-ph].
- [32] D. B. Hume, C. W. Chou, T. Rosenband, and D. J. Wineland, *Phys. Rev. A* **80**, 052302 (2009).
- [33] C. Wu, C. Guo, Y. Wang, G. Wang, X.-L. Feng, and J.-L. Chen, *Phys. Rev. A* **95**, 013845 (2017).
- [34] K. D. B. Higgins, S. C. Benjamin, T. M. Stace, G. J. Milburn, B. W. Lovett, and E. M. Gauger, *Nature Communications* **5**, 1 (2014).
- [35] Y. Zhao, R. Zhang, W. Chen, X.-B. Wang, and J. Hu, *npj Quantum Information* **7**, 24 (2021).
- [36] D. M. Greenberger, M. A. Horne, and A. Zeilinger, “Go-

- ing beyond bell's theorem," in *Bell's Theorem, Quantum Theory and Conceptions of the Universe*, edited by M. Kafatos (Springer Netherlands, Dordrecht, 1989) pp. 69–72.
- [37] J. J. . Bollinger, W. M. Itano, D. J. Wineland, and D. J. Heinzen, *Phys. Rev. A* **54**, R4649 (1996).
- [38] T. Monz, P. Schindler, J. T. Barreiro, M. Chwalla, D. Nigg, W. A. Coish, M. Harlander, W. Hänsel, M. Hennrich, and R. Blatt, *Phys. Rev. Lett.* **106**, 130506 (2011).
- [39] M. Kitagawa and M. Ueda, *Phys. Rev. A* **47**, 5138 (1993).
- [40] T. Holstein and H. Primakoff, *Phys. Rev.* **58**, 1098 (1940).
- [41] D. C. Liu and J. Nocedal, *Mathematical Programming* **45**, 503 (1989).
- [42] J. Bezanson, A. Edelman, S. Karpinski, and V. B. Shah, *SIAM Review* **59**, 65 (2017).
- [43] P. K. Mogensen and A. N. Riseth, *Journal of Open Source Software* **3**, 615 (2018).
- [44] I. Apellaniz, B. Lücke, J. Peise, C. Klempt, and G. Tóth, *New Journal of Physics* **17**, 083027 (2015).
- [45] Y. Ouyang, N. Shettell, and D. Markham, *IEEE Transactions on Information Theory* **68**, 1809 (2022).
- [46] P. W. Shor, *Physical review A* **52**, R2493 (1995).
- [47] K. Mølmer and A. Sørensen, *Phys. Rev. Lett.* **82**, 1835 (1999).
- [48] K. Kim, M.-S. Chang, R. Islam, S. Korenblit, L.-M. Duan, and C. Monroe, *Phys. Rev. Lett.* **103**, 120502 (2009).
- [49] J. Britton, B. C. Sawyer, C.-C. J. W. A. C. Keith, J. Freericks, H. Uys, M. J. Biercuk, and J. J. Bollinger, *Nature* **484**, 489 (2012).
- [50] J. Zhang, G. Pagano, P. W. Hess, A. Kyprianidis, P. Becker, H. Kaplan, A. V. Gorshkov, Z.-X. Gong, and C. Monroe, *Nature* **551**, 601 (2017).
- [51] G. Kirchmair, J. Benhelm, F. Zähringer, R. Gerritsma, C. F. Roos, and R. Blatt, *New Journal of Physics* **11**, 023002 (2009).
- [52] A. Sørensen and K. Mølmer, *Phys. Rev. A* **62**, 022311 (2000).
- [53] W. Ge, B. C. Sawyer, J. W. Britton, K. Jacobs, J. J. Bollinger, and M. Foss-Feig, *Phys. Rev. Lett.* **122**, 030501 (2019).
- [54] Y. Shapira, R. Shaniv, T. Manovitz, N. Akerman, L. Peleg, L. Gazit, R. Ozeri, and A. Stern, *Phys. Rev. A* **101**, 032330 (2020).
- [55] J. D. Arias Espinoza, K. Groenland, M. Mazzanti, K. Schoutens, and R. Gerritsma, *Phys. Rev. A* **103**, 052437 (2021).
- [56] N. Gutman, A. Gorlach, O. Tziperman, R. Ruimy, and I. Kaminer, "Universal control of symmetric states using spin squeezing," (2023), arXiv:2312.01506 [quant-ph].